# Prediction of the tertiary structure of a caspase-9/inhibitor complex

Kuo-Chen Chou[a],*, Alfredo G. Tomasselli[b], Robert L. Heinrikson[b]

[a]*Computer-Aided Drug Discovery, Pharmacia and Upjohn, Kalamazoo, MI 49007-4940, USA*
[b]*Protein Science, Pharmacia and Upjohn, Kalamazoo, MI 49007-4940, USA*

**Abstract** Apoptosis, or programmed cell death, plays a central role in the development and homeostasis of an organism. The breakdown of cellular proteins in apoptosis is mediated by caspases, which comprise a highly conserved family of cysteine proteases with specificity for aspartic acid residues at the P1 positions of their substrates. Multiple lines of evidence show that caspase-9 is critical for an apoptosis pathway mediated via the mitochondria. In this study, the three-dimensional structure of the catalytic domain of caspase-9 and its interaction with the inhibitor acetyl-Asp-Val-Ala-Asp fluoromethyl ketone (Ac-DVAD-fmk) have been predicted by a segment matching modeling procedure. As expected, the predicted caspase-9 structure shows both a high similarity in the overall folding topology and remarkable differences in the surface loop regions as compared to other caspase family members such as caspase-1, -3 and -8, for which crystal structures have been determined. This kind of comparative analysis reflects the convergence–divergence duality among the caspases. Moreover, some subtle differences have been observed between caspase-9 and caspase-3 in the subsite contacts with the covalently linked inhibitor Ac-DVAD-fmk. Based on the X-ray structural analysis of caspase-8, a main chain carbonyl oxygen appears to be involved in a catalytic triad with the active site Cys and His residues. The corresponding carbonyl oxygen in caspase-9, together with other expected features of the catalytic apparatus, appears in our model. The predicted structure of caspase-9 can serve as a reference for subsite analysis relative to rational design of highly selective caspase inhibitors for therapeutic application.
© 2000 Federation of European Biochemical Societies.

*Key words:* Apoptosis; Caspase-1; Caspase-3; Caspase-8; Catalytic Cys-His-$X_{bkO}$ triad; Convergence–divergence duality

## 1. Introduction

Apoptosis, also known as programmed cell death or cellular suicide, plays a central role in development and homeostasis of an organism [1,2] and is currently an area of intense investigation. Unlike human beings committing suicide that almost always leads to a tragedy, the normal function of cellular suicide within the organism is vital to life. It serves to prune tissues during embryonic development and provides a mechanism for removal of damaged cells in the adult in a neat,

orderly way. In normal animal development, cell death is involved not only in morphogenesis, but also in optimizing function in the immune and central nervous systems. Cell death and renewal are responsible for maintaining the proper turnover of cells, which ensures a constant controlled flux of fresh cells. Programmed cell death and cell proliferation are tightly coupled. When apoptosis malfunctions, a variety of formidable diseases can ensue: blocking apoptosis is associated with cancer [3,4] and autoimmune diseases, while unwanted apoptosis can possibly lead to ischemic damage [5–7] or neurodegenerative disease [8–10]. Apoptosis is considered to play a key role in these several devastating diseases and, in principle, provides many targets for therapeutic intervention [11].

The question as to how cells die in an organized, non-necrotic fashion has intrigued biologists for decades. Most apoptotic processes are mediated through caspases although caspase-independent apoptosis does exist [12,13]. The activation of caspases (cysteinyl aspartate-specific proteases) is a key event in the induction of programmed cell death, as it initiates a cascade of cleavage reactions that contribute to the disruption of structural components within the cell, as well as the disabling of critical repair processes. While detailed structural analyses have not been performed for all caspases, amino acid sequence alignments demonstrate that caspases comprise a highly conserved family of cysteine proteases with specificity for aspartic acid residues in their substrates [14–17]. It is the cleavage of key substrates by these caspases that orchestrates the organized and efficient packaging of the cells for clearance. Accordingly, apoptosis is actually a process of caspase-mediated cell death. In view of this, caspase inhibitors might represent effective new drugs against Alzheimer's disease, and other incurable degenerative disorders where it is desirable to block apoptosis [18]. The rational design of such caspase inhibitors will require detailed structural information concerning their catalytic sites and modes of ligand binding.

The three-dimensional (3-D) structures of caspase-1 (also called interleukin converting enzyme (ICE)) and caspase-3 (also called apopain or CPP32) have been determined by X-ray crystallography [19–21]. The 3-D structure of caspase-8 (also called FLICE) was first predicted by computer modeling [22], and later determined at atomic resolution by X-ray crystallography [23,24]. The predicted 3-D structure of caspase-8 and the corresponding X-ray structure are very close, especially in the core of the structure (root mean square deviation (RMS) = 1.2 Å).

Caspase-9 is another of the initiating, or upstream activator caspases which lead to production of the downstream executioners of apoptosis such as caspase-3. However, the 3-D structure of caspase-9 has not as yet been reported. Although

---

*Corresponding author. Fax: (1)-616-372 8766.
E-mail: kuo-chen.chou@am.pnu.com

caspase-8 can lead directly to downstream caspase activation in certain cell types, and with appropriate death stimuli, mitochondria are the essential mediators in others [25]. Actually, mitochondrial damage is a major amplification step in the apoptotic pathway [26], and caspase-9 is the central initiator that works in conjunction with cytochrome *c*, Apaf-1 and dATP to activate the downstream caspases-3, -6 and -7 [27,28]. Recently, a model for caspase-9 recruitment to the Apaf-1 complex via caspase recruitment domain (CARD)/CARD interactions was derived, based on the nuclear magnetic resonance (NMR)-determined CARD structure of the RIP-associated ICH-1 with a death domain (RAIDD) adaptor protein [28,29]. Interestingly, multiple lines of evidence show that caspase-9 activation also serves as an amplification step in the Fas/TNF-induced apoptosis pathway via caspase-8. Upon cleavage by caspase-8, BID, a pro-apoptosis regulatory protein, is able to induce cytochrome *c* release and thereby activate caspase-9 [26,30]. The 3-D solution structure of BID [31] and the solution structure of Apaf-1 CARD and its interaction with caspase-9 CARD [32] were recently determined by NMR. A recent report further confirms that caspase-9 is critical for cytochrome *c*-dependent apoptosis and normal brain development [6]. Although the details of how

procaspase-9 becomes activated are not known, mutations in caspase-9 result in embryonic lethality with a much enlarged and malformed cerebrum similar to that seen in caspase-3 knockout mice [33,34]. In view of the importance of the caspase-9 pathway in mediating the apoptotic response, it is of considerable interest to gain insights into the tertiary structure of this enzyme. The current study describes the modeling of the 3-D structure of the protease domain of caspase-9 in complexation with the inhibitor acetyl-Asp-Val-Ala-Asp fluoromethyl ketone (Ac-DVAD-fmk).

## 2. Materials and methods

The sequence of caspase-9 (also called ICE-LAP6) was taken from Duan et al. [35] and Srinivasula et al. [36]. It was found by running a BLAST search [37,38] that, among proteins of known 3-D structure, caspase-3 had the highest score bits in sequence similarity with caspase-9. It was indicated by running BESTFIT in the GCG package [39] that the sequence similarity between the two enzymes was 50.7%. Accordingly, the X-ray structure of caspase-3 determined by Mittl et al. [21] was selected as a template to predict the 3-D structure of caspase-9. The sequences of caspase-3 and caspase-9 were aligned using the PILEUP program in the GCG package [39]. The aligned result is given in Fig. 1, where the amino acid sequences in black boxes represent the protease domain whose atomic coordinates were

```
Caspase-3    ~~~~~~~~~~  ~~~~~~~~~~  ~~~~~~~~~~  ~~~~~~~~~~  ~~~~~~~~~~
Caspase-9    MDEADRRLLR  RCRLRLVEEL  QVDQLWDVLL  SRELFRPHMI  EDIQRAGSGS


Caspase-3    ~~~~~~~~~~  ~~~~~~~~~~  ~~~~~~~~~~  ~~~~~~~~~~  ~~~~~~~~~~
Caspase-9    RRDQARQLII  DLETRGSQAL  PLFISCLEDT  GQDMLASFLR  TNRQAGKLSK


Caspase-3    ~~~~~~~~~~  ~~~~~~~~~~  ~MENTENSVD  SKSIKNLEPK  IIHGSESMDS
Caspase-9    PTLENLTPVV  LRPEIRKPEV  LRPETPRPVD  IGSGGFGD..  .VGALESLRG

                     35                                              79
                     ↑                                               ↑
Caspase-3    GISLD NSYKM  DYPEMGLCII  INNKNFHKST  GMTSRSGTDV  DAANLRETFR
Caspase-9    ..NAD LAYIL  SMEPCGHCLI  INNVNFCRES  GLRTRTGSNI  DCEKLRRRFS
                   ↓                                              ↓
                   151                                            195
             80                                           124
             ↑                                            ↑
Caspase-3    NLKYEVRNKN  DLTREEIVEL  MRDVSKEDHS  KRSSFVCVLL  SHGEE.....
Caspase-9    SLHFMVEVKG  DLTAKKMVLA  LLELARQDHG  ALDCCVVVIL  SHGCQASHLQ
             ↓                                              ↓
             196                                            245
                 125                                        171
                 ↑                                          ↑
Caspase-3    ..GIIFGTNG  .PVDLKKITN  FFRGDRCRSL  TGKPKLFIIQ  ACRGTELDCG
Caspase-9    FPGAVYGTDG  CPVSVEKIVN  IFNGTSCPSL  GGKPKLFFIQ  ACGGEQKDHG
                                                                   ↓
                                                                   295
             173                                     185        197
             ↑                                       ↑          ↑
Caspase-3    IE TDSGVDDD  M.........  ..........  .....AC HKI  PVDADFLYAY
Caspase-9    FE VASTSPED  ESPGSNPEPD  ATPFQEGLRT  FDQLDAI SSL  PTPSDIFVSY
             ↓                                       ↓          ↓
             297                                     333        345
                                                               247
Caspase-3    STAPGYYSWR  NSKDGSWFIQ  SLCAMLKQYA  DKLEFMHILT  RVNRKVATEF
Caspase-9    STFPGFVSWR  DPKSGSWYVE  TLDDIFEQWA  HSEDLQSLLL  RVANAVSVKG
                                                                   ↓
                                                                   395
                                        277
                                        ↑
Caspase-3    ESFSFDATFH  AKKQIPCIVS  MLTKELYFYH
Caspase-9    IYKQMPGCFN  FLRKKLFFKT  S~~~~~~~~~
                                       ↓
                                       416
```
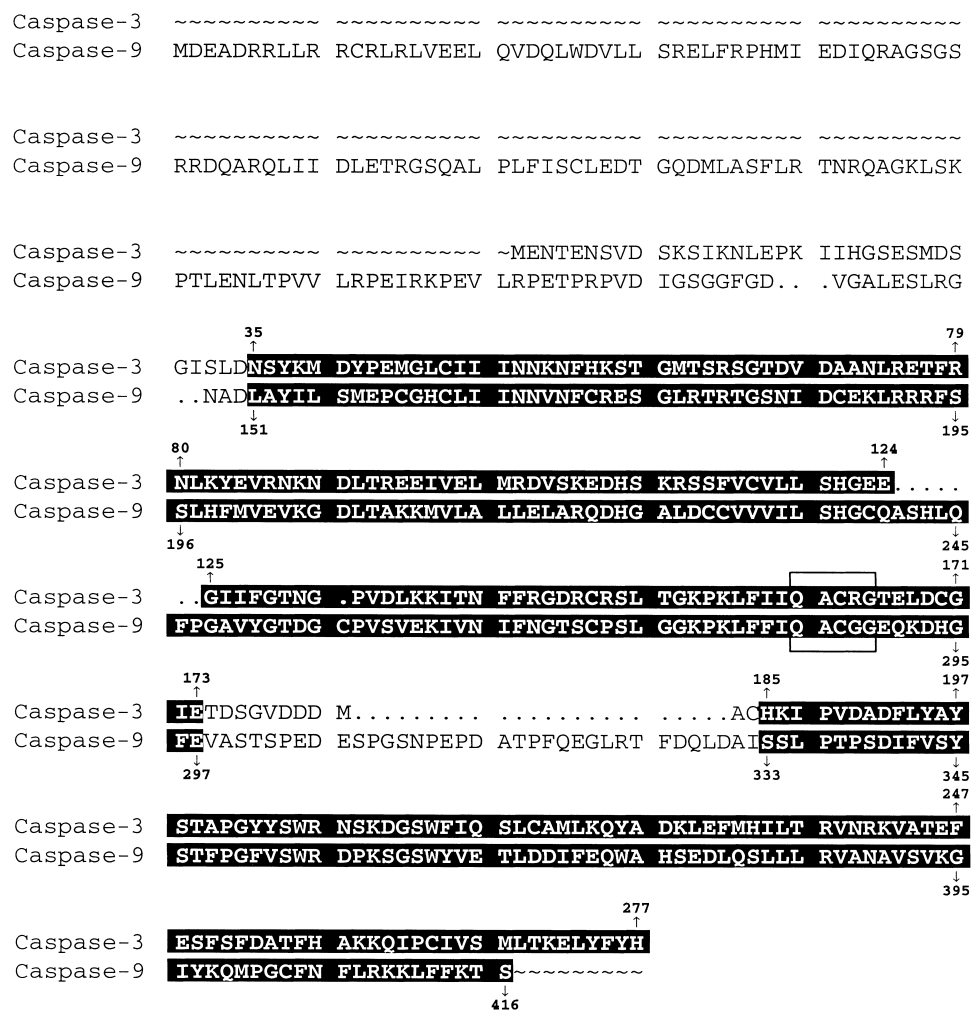
Fig. 1. Alignment of the amino acid sequences of caspase-3 and caspase-9 using PILEUP in the GCG package [39]. The amino acids in the black box for caspase-3 are defined by X-ray coordinates [21]; those for caspase-9 are predicted in the present study. The amino acids bracketed are the conserved active site pentapeptide segments for the caspase family [48,49].
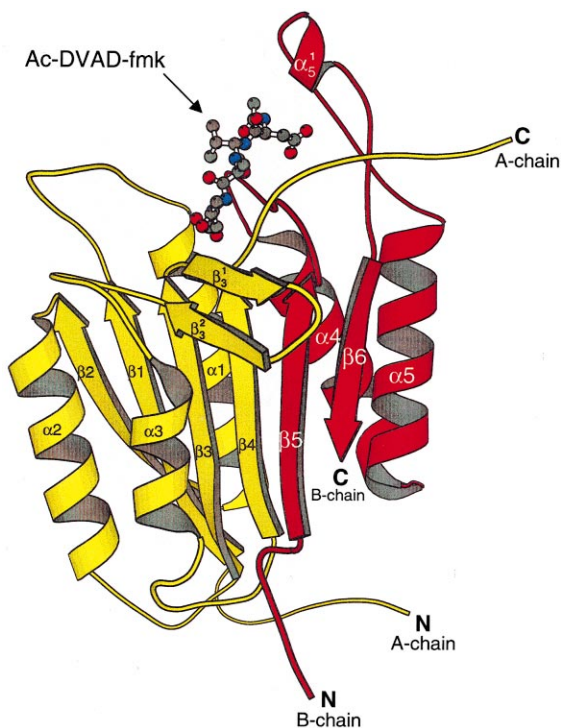
Fig. 2. Schematic representation of the caspase-9:Ac-DVAD-CH$_2$ complex. The ribbon drawing is used for the heterodimer enzyme, where the A-chain is colored yellow and the B-chain burgundy. The inhibitor is represented by a ball and stick drawing.

either determined by X-ray crystallography, as for the case of caspase-3 [21], or are to be predicted as done here for caspase-9. In the domain comparisons, the A- and B-chains of caspase-3 comprise residues 35–173 and residues 185–277, respectively, and for caspase-9, residues 151–297 and 332–405, respectively.

Based on the sequence alignment (Fig. 1) and the X-ray coordinates of caspase-3, the protease domain of caspase-9 was predicted. Meanwhile, based on the coordinates of the tetrapeptide Ac-DVAD-CH$_2$ in the caspase-3:Ac-DVAD-CH$_2$ complex, the binding site of the inhibitor to caspase-9 was also located. In the present study, the segment matching modeling method [40] was adopted to compute the protease domain of caspase-9. This method uses a database of known protein structures to build an unknown target structure from the amino acid sequence. The target structure is first broken into a set of short segments. The database is then searched for matching segments on the basis of amino acid sequence similarity and compatibility with the target structure. The process is repeated 10 times and an average model is generated, followed by energy minimization to create the final model. This procedure was originally shown to be highly accurate for eight test proteins ranging in size from 46 to 323 residues, where the all-atom RMS deviation of the modeled structures is between 0.93 Å and 1.73 Å [40]. This method was used to model the structure of the protease domain of caspase-8 at a time before the X-ray coordinates were released for caspase-3 [22]. First, the atomic coordinates of the catalytic domain of caspase-3 were predicted based on the X-ray structure of caspase-1, and then the caspase-3 structure thus obtained served as a template to model the protease domain of caspase-8. After the X-ray coordinates of caspase-3 protease domain were finally released and the X-ray structure of the caspase-8 protease domain determined [23], it turned out that the RMS for all the backbone atoms of the caspase-3 protease domain between the X-ray and predicted structures is 2.7 Å, and the corresponding RMS is 3.1 Å for caspase-8 and only 1.2 Å for its core structure. This indicates that the computed structures of caspase-3 and -8 were quite close to the corresponding X-ray structures. Recently, this method was applied to model the CARDs of Apaf-1, caspase-9, Ced-4 and Ced-3, based on the NMR structure of the RAIDD CARD [29], and for TPKII (Tau protein kinase) [41] based on the X-ray structure of the Cdk2–cyclin A–ATP complex.

The computed structure now obtained for caspase-9 was further refined by energy minimization with respect to all the side-chains using AMBER (assisted model building with energy refinement) force field [42]. An examination by ProCheck [43] for the current model has indicated its rationality from the structural point of view.

## 3. Results and discussion

The predicted 3-D structure of caspase-9 is illustrated in Fig. 2.

### 3.1. Overall structure

The structure of caspase-9 consists of the A-chain (yellow) and B-chain (burgundy) comprising residues 151–297 and 333–416, respectively (Figs. 1 and 2). The two polypeptide chains associate to form a heterodimer, which folds into one compact structure of a single domain with an overall dimension of ∼26 Å×37 Å×39 Å and a solvent accessible surface of ∼11 918 Å$^2$. The two subunits interact extensively and are tethered to each other by 28 hydrogen bonds. The approximate area of the solvent accessible interface between the two subunits is 3590 Å$^2$. As expected, the overall topology is similar to that of caspase-1, caspase-3 and caspase-8, with a typical α/β folding motif. The core of the enzyme is formed by a central 6-stranded β-sheet (Fig. 2), of which four strands (β1, residues 160–168; β2, 199–206; β3, 228–236; β4, 279–286) are donated from the A-chain and two (β5, residues 340–347; β6, 411–416) from the B-chain. Except for β6, the first five strands are all parallel. Consistent with the handedness of β-sheets observed in proteins [44], the β-sheet in the predicted caspase-9 structure assumes a right-handed twist, a result dictated by energetic optimization [45,46]. The β-sheet is surrounded by five α-helices: two (α2, residues 208–222; α3, 259–268) are located on one side of the sheet, and three (α1, residues 182–198; α4, 361–377; α5, 379–393) on the oth-
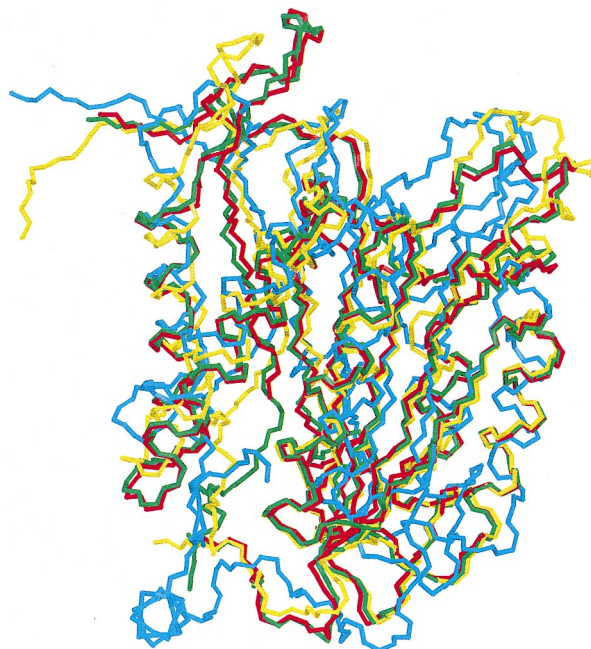


Fig. 3. A backbone superimposition of the X-ray crystallographic structures of caspase-1 (blue), caspase-3 (green) and caspase-8 (yellow), and our predicted structure of caspase-9 (red).
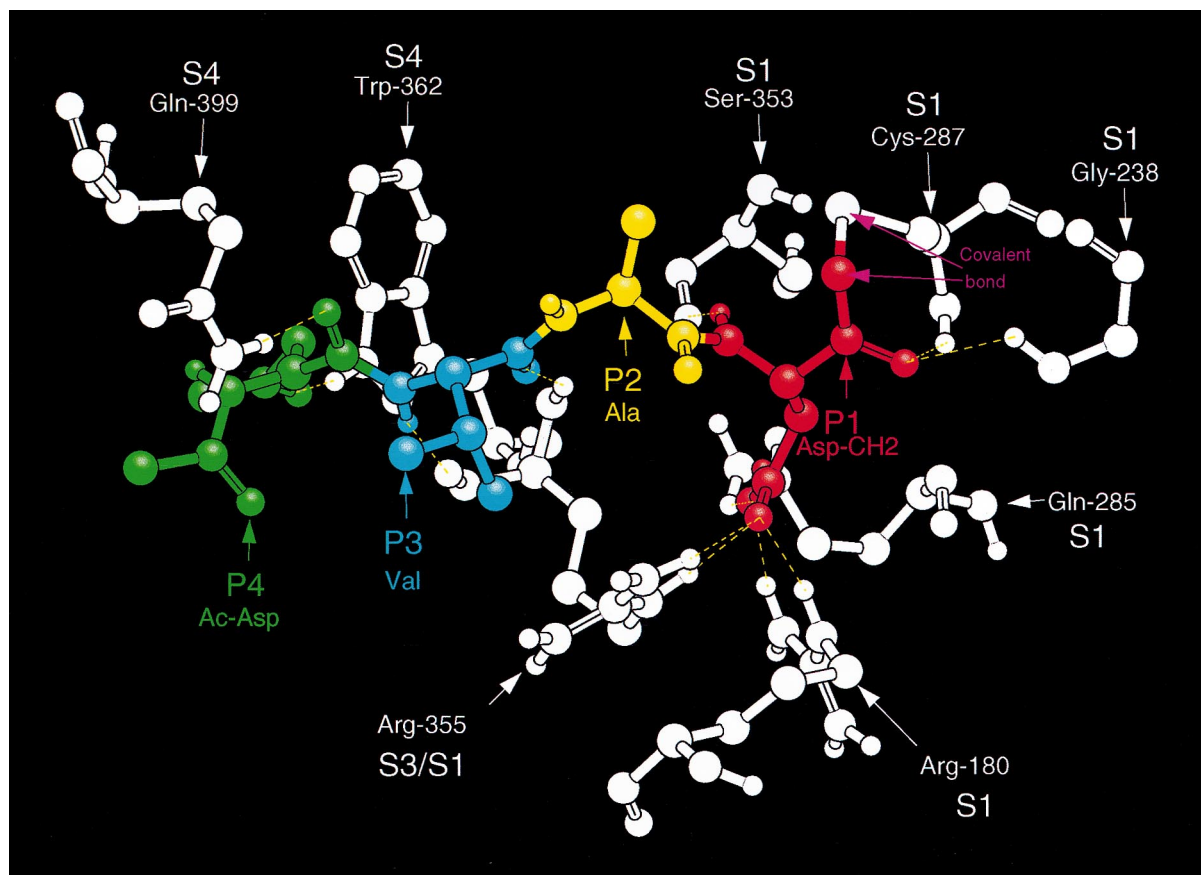
Fig. 4. The binding interaction between the covalently bound inhibitor Ac-DVAD-CH$_2$ and caspase-9. P1, P2, P3 and P4 residues of the inhibitor are colored red, yellow, light blue and green, respectively. The relevant residues of the enzyme are colored white; hydrogen bonds are represented by yellow dotted lines. The interaction is featured by a covalent thioether bond between the methylene C of the P1 Asp residue and S-γ of Cys-287, as well as the 12 hydrogen bonds as detailed in Table 1. Only heavy atoms and the hydrogen atoms attached to the hetero-atoms are shown.

er side. Helices α1, α2 and α3 belong to the A-chain, and helices α4 and α5 to the B-chain. The loop between β3 and α3 contains a minor β-sheet formed by two short antiparallel β-strands, $β_3^1$ (residues 238–242) and $β_3^2$ (residues 246–250). The loop between α5 and β6 contains a very short α-helix, $α_3^1$ (residues 402–405). As is the case with other caspase family members, the C-terminus of the A-chain and the N-terminus of the B-chain lie at opposite ends of the molecule (Fig. 2); these segments appear to play a role in the formation of protease heterotetramers.

Finally, to provide an overall illustration of the general similarity and subtle differences among the 3-D structures of caspase-1, caspase-3, caspase-8 and caspase-9, a backbone superimposition of the four enzymes is given in Fig. 3, where caspase-1 is colored blue, caspase-3 green, caspase-8 yellow and caspase-9 red. As we can see from the superimposed picture, although the general folding topology of the four structures is quite similar, there are many differences in their surface loop regions that are actually caused by the existence of insertions or deletions in amino acids [22]. Just as in the

Table 1
Hydrogen bond interactions between caspase-9 and Ac-DVAD-CH$_2$

| Subsite[a] | Atom in Ac-DVAD-CH$_2$ | Atom in caspase-9 | Distance (Å) |
|---|---|---|---|
| S4 | Asp-1 O-δ1 | Trp-362 N-ε | 2.64 |
| | Asp-1 O | Gln-399 N-ε2 | 2.70 |
| S3 | Val-2 N | Arg-355 O | 2.95 |
| | Val-2 O | Arg-355 N | 2.84 |
| S2 | | | |
| S1 | Asp-4 O-δ1 | Arg-180 N-ε | 2.81 |
| | Asp-4 O-δ2 | Arg-180 N-η2 | 2.82 |
| | Asp-4 O | Gly-238 N | 3.02 |
| | Asp-4 O-δ2 | Gln-285 N-ε2 | 2.74 |
| | Asp-4 O | Cys-287 N | 3.32 |
| | Asp-4 N | Ser-353 O | 2.98 |
| | Asp-4 N | Arg-355 O | 2.95 |
| | Asp-4 O | Arg-355 N | 2.84 |

[a]The subsite symbol and order proposed by Schechter and Berger [48] are adopted here.

case of lectin domains in the selectin family [47], this kind of similarity and difference reflects the convergence–divergence duality in the catalytic domains of the caspase family. Particularly, it is the difference in the loop regions near the active site that may be of use for rationally designing caspase inhibitors with a highly selective specificity.

### 3.2. Inhibitor binding

Right above the end of the β4 strand (Fig. 2), there is a deep cavity of $\sim 9$ Å $\times 8$ Å $\times 16$Å, where the tetrapeptide inhibitor moiety, acetyl-Asp-Val-Ala-Asp-CH$_2$, is bound to the active site thiol of the enzyme. The approximate area of the solvent accessible interface between the enzyme and the inhibitor is 864 Å$^2$. The detailed binding interaction between the predicted caspase-9 catalytic domain and the tetrapeptide inhibitor is shown in Fig. 4, where the hydrogen bonds between the enzyme and the inhibitor are shown by the yellow dotted lines and the two atoms that form the irreversible covalent bond (the thioether bond) by two pink arrows. There are a total of 12 hydrogen bonds that tether the inhibitor to the enzyme. An examination of the binding interaction for each of the four subsites of the tetrapeptide inhibitor led to the following information (the subsite symbol and order follow the expression proposed originally by Schechter and Berger [48]). (1) S4 pocket: there are two hydrogen bonds that tether the first residue of the tetrapeptide inhibitor, Asp-1 or P4, to the residues Trp-362 and Gln-399 of the enzyme. (2) S3 pocket: two hydrogen bonds are formed that hold the P3 Val-2 to Arg-355 of the enzyme. (3) S2 pocket: there is no hydrogen bond between the third residue of the inhibitor, Ala-3 or P2, and the enzyme, which is exactly the same as observed in the X-ray structure for the caspase-3:inhibitor complex [21]. This is very likely due to the small size of the Ala side-chain. If the P2 Ala is replaced with a large side-chain residue, such as in the caspase-3:Ac-DEVD-CH$_2$ complex, two hydrogen bonds have been observed that tether Val-3 to the enzyme [20]. (4) S1 pocket: the most hydrogen bonds are formed in
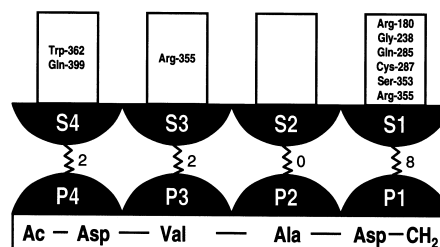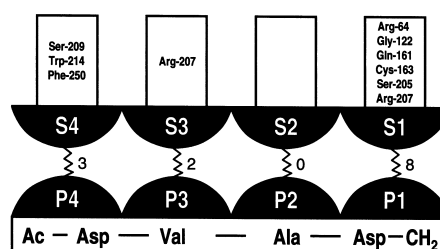


Fig. 5. A schematic illustration of the similarity and difference of the hydrogen bonding interaction with the tetrapeptide inhibitor Ac-DVAD-CH$_2$ in (a) caspase-9 complex and (b) caspase-3 complex. Counterparts of the inhibitor P1–P4 residues are represented by the enzyme subsites, S1, S2, S3 and S4, respectively. Each of such four S–P pairs has a zigzag line with a figure to indicate the number of the corresponding hydrogen bonds therein. Residues in S1 and S3 are spatially equivalent in the two enzymes; in S4, only the Trp residues are equivalent.

this pocket, just as in the case of caspase-3:inhibitor complex [21]. There are eight hydrogen bonds formed in this pocket that tether the fourth residue of the tetrapeptide inhibitor, Asp-4 or P1, to the residues Arg-180, Gly-238, Gln-285, Cys-287, Ser-353 and Arg-355 of the enzyme. As shown in

Table 2
Hydrogen bond interactions between the amino acids in the conservative pentapeptide QACXG and the other part of the enzyme for each of the four caspase members

| Caspase member | Atom in the amino acid in the conservative QACXG pentapeptide | Atom in the other part of the enzyme | Distance (Å) |
|---|---|---|---|
| Caspase-1, **X = Arg-286** | Gln-283 N | Phe-234[a] O | 3.05 |
| | Gln-283 O | Ser-236[b] N | 2.85 |
| | **Arg-286** N | Glu-390 O-ε2 | 2.18 |
| Caspase-3, **X = Arg-164** | Gln-161 N | Leu-118[a] O | 3.01 |
| | Gln-161 O | Ser-120[b] N | 3.14 |
| | Gln-161 N-ε2 | Ser-205 O-γ | 2.65 |
| | **Arg-164** O | Gly-202 N | 2.64 |
| | **Arg-164** N | Tyr-203[c] O | 3.00 |
| | **Arg-164** N-η2 | Glu-124[d] O-ε2 | 2.86 |
| Caspase-8, **X = Gln-361** | Gln-358 N | Ile-314[a] O | 2.83 |
| | Gln-358 O | Ser-316[b] N | 2.94 |
| | **Gln-361** N-ε2 | Ile-322 O | 2.98 |
| | **Gln-361** N-ε2 | Cys-360 O | 2.93 |
| | **Gln-361** O-ε1 | Gly-321 N | 2.93 |
| Caspase-9, **X = Gly-288** | Gln-285 N | Ile-234[a] O | 2.88 |
| | Gln-285 O | Ser-236[b] N | 2.96 |
| | Gln-285 O-ε1 | Lys-410 N-ζ | 2.77 |
| | Ala-286 N | Ser-346 O-γ | 2.75 |
| | **Gly-288** N | Phe-351[c] O | 2.93 |
| | **Gly-288** O | Gln-240[d] N-ε2 | 2.72 |

Amino acid residues with a same superscript are equivalent to one another in position according to the sequence alignment of the four caspases (see Figs. 1 and 3 of Chou et al. [22] and Fig. 1 of this paper).
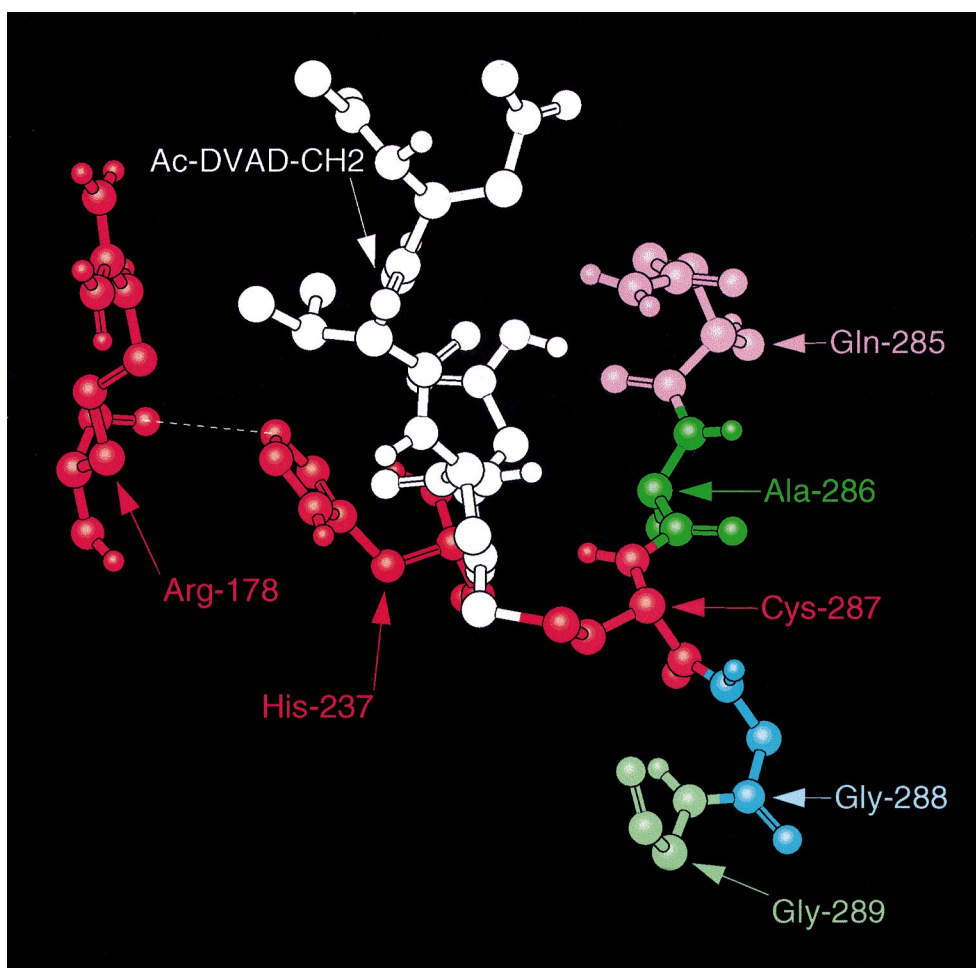
Fig. 6. Illustration to show the relative position of the inhibitor Ac-DVAD-CH$_2$, the conserved pentapeptide QACGG and the catalytic triad of caspase-9. The inhibitor is colored white, and the three components of the catalytic triad are highlighted by red. The dotted line is used to mark the 2.78 Å distance between the backbone carbonyl oxygen of Arg-178 and the N-ε2 of His-237. Only heavy atoms and the hydrogen atoms attached to the hetero-atoms are shown.

Fig. 4 and Table 1, Arg-355 alone contributes four hydrogen bonds in binding the inhibitor: two for P3 and two for P1. Accordingly, Arg-355 could be an excellent candidate for mutagenesis studies. The detailed atom pairs that are involved in forming these hydrogen bonds and their distances are given in Table 1. To facilitate the comparison between caspase-9 and caspase-3 in inhibitor binding, the hydrogen bonding interaction between the inhibitors and the enzymes in each of the four subsites is shown schematically in Fig. 5a,b. As we can see from Fig. 5, although some differences exist between caspase-9 and caspase-3 in the S4 subsite, the interactions in S3, S2 and S1 are identical. Also, as in the case of the caspase-3:inhibitor complex [21], there is an alkyl thioether bond, that tightly binds the methylene carbon of the P1 Asp to Cys-287 of the enzyme. The distance predicted between this methylene carbon atom of the inhibitor and the atom S-γ of Cys-287 of the enzyme is 1.81 Å, which is exactly the same as that seen in the X-ray structure of the caspase-3:inhibitor complex.

### 3.3. The conserved pentapeptide segment QACXG

The pentapeptide segments as bracketed in Fig. 1 is highly conserved among caspase family members as generally expressed by QACXG [36,49]. For caspase-1 and -3, it is

QACRG, for caspase-8, QACQG, and for caspase-9, QACGG. As pointed out by Alnemri [50], while the overall amino acid sequence identity varies from about 25% to 55% among caspases, the active sites of all caspase family members contain the conserved pentapeptide sequence QACXG, suggesting that the catalytic mechanism is conserved. It is interesting to note that among all known caspases to date, only caspase-9 has a Gly residue as X in the pentapeptide sequence. The absence of a side-chain at this position in caspase-9 suggests more flexibility in the active site region and, indeed, more access to conformational space. It is of interest, therefore, to note the environment of the QACXG region, and in particular of the X-residue, in the various solved caspase structures. In Table 2 is given an array of H-bond contacts seen in the QACXG residues in the three solved caspase/inhibitor complexes, and in the predicted caspase-9 structure. The first Gln residue shows identical interactions in caspase-1, -3 and -8 involving amide to carbonyl H-bonds; these are formed among homologous regions in the chains. These same interactions are predicted in caspase-9. In caspase-3, the Gln amide is hydrogen-bonded to the side-chain oxygen of Ser-205. We predict a different additional H-bond involving the side-chain carbonyl oxygen of the Gln and the N-ε of Lys-

410. The Cys and final Gly of the conserved pentapeptide sequence show no differences among the four caspases. Of interest is the Ala, which in our caspase-9 model alone shows a H-bond interaction between the amide and the O-γ of Ser-346. Located two residues away is the X-residue, a Gly in caspase-9. Since the pentapeptide QACXG has an extended conformation, the side-chains of every other residues along the peptide, such as A and X, are even closer than those of two consecutive ones. Thus, the absence of a side-chain at the residue X, Gly-288, provides a space for access of the side-chain of Ser-346 to form a hydrogen bond with Ala-286, which is an unique feature for caspase-9. The X-residue in caspase-9, Gly-288, is pinned down by two H-bonds involving its main chain amide and carbonyl oxygen; the former is with the carbonyl oxygen of Phe-351. This corresponds to a similar H-bond seen in the X-residue of caspase-3, i.e. Arg-164, in which the main chain amide is linked to the carbonyl oxygen of the homologous Tyr-203. Interactions seen between the side-chains of the X-residues and portions of the respective enzymes are variable and difficult to interpret. A general picture does not emerge from the structural comparisons, but it would appear that the space around the fourth Gly residue in the caspase-9 model can be partially filled by the insertion of the side-chains of Ser-346 and Thr-347. These changes may, therefore, represent a compensation for the small X-residue in caspase-9.

### 3.4. A catalytic triad

Wilson et al. [19] proposed the Cys-His catalytic dyad for caspase-1, but indicated the possible involvement of a putative third component, the backbone carbonyl oxygen of Pro-177, that could affect the basicity of the histidine imidazole. For the case of caspase-3, Rotonda et al. [20] invoked the existence of the same carbonyl oxygen of Thr-62 that might play the same role as that of Pro-177 in caspase-1. Since no clear evidence was provided about the third component, Mittl et al. [21] suggested that the ICE-like proteases have a catalytic Cys-His dyad instead of the classical Cys-His-Asn triad as found in papain and most other cysteine proteases. Recently, based upon the atomic resolution structure of caspase-8, it was observed [23] that the distance between the carbonyl oxygen of Arg-258 and the N-ε2 of His-317 is 2.74 Å, which is smaller than 3 Å and hence indicates a clear interaction between these two atoms. Arg-258 in caspase-8 is equivalent to Pro-177 in caspase-1 and Thr-62 in caspase-3. Accordingly, Watt et al. [23] inferred that, irrespective of the nature of the amino acid at this position, the carbonyl oxygen can serve as a member of a catalytic triad in the caspases. Actually, even in the earlier computed structure [22] of caspase-8, it was found that the distance between the carbonyl oxygen of Arg-258 and the N-ε2 of His-317 is 2.96 Å (i.e. also < 3 Å), suggesting a possible salt bridge interaction as well. The current model of caspase-9 further supports such an inference. As shown in Fig. 6, the distance between the carbonyl oxygen of Arg-178 and N-ε2 of His-237 is 2.78 Å, implying that the carbonyl oxygen of Arg-178 can serve as a member of a catalytic triad in the caspase-9. According to the sequence alignment of Fig. 1 as well as the sequence alignments of Figs. 1 and 3 in Chou, K.C. et al. [22], Arg-178 of caspase-9 is equivalent to Pro-177 of caspase-1, Thr-62 of caspase-3 and Arg-258 of caspase-8; while His-237 in caspase-9 is equivalent to His-237 in caspase-1, His-121 in caspase-3 and His-317 in

caspase-8. Except for the structure determined by Wilson et al. [19] for caspase-1, in which the distance between the carbonyl oxygen of Pro-177 and N-ε2 of His-237 is 3.24ε, the corresponding distances for all the other three caspases are less than 3 Å. It is anticipated that by improving the resolution in determining the X-ray structure, such a distance in caspase-1 might also fall within the range of 3 Å. Therefore, it appears likely that caspases utilize a catalytic Cys-His-$X_{bkO}$ triad mechanism, where $X_{bkO}$ represents the backbone carbonyl oxygen of any residue at the position of the third component of the triad, irrespective of the nature of the amino acid concerned: for caspase-1, it is Pro-177; for caspase-3, Thr-62; for caspase-8, Arg-258; and for caspase-9, Arg-178.

Since caspase-9 has become increasingly important in the study of apoptosis, the 3-D structure of caspase-9 as reported here will further stimulate the study of this area. Particularly, it can serve as a footing for thinking about design of inhibitors.

## References

[1] Raff, M. (1998) Nature 396, 119–122.
[2] Jacobson, M.D., Weil, M. and Raff, M.C. (1997) Cell 88, 347–354.
[3] Evan, G. and Littlewood, T. (1998) Science 281, 1317–1322.
[4] Adams, J.M. and Cory, S. (1998) Science 281, 1322–1326.
[5] Narula, J., Panday, P., Arbstini, E., Haider, N., Narula, N., Kolodgie, F.D., Dal Bello, B., Semigran, M.J., Bielsa-Masdeu, A., Dec, G.W., Israels, S., Ballester, M., Virmani, R., Saxena, S. and Kharbanda, S. (1999) Proc. Natl. Acad. Sci. USA 96, 8144–8149.
[6] Krajewski, S., Krajewska, M., Ellerby, L.M., Welsh, K., Xie, Z., Deveraux, Q.L., Salvesen, G.S., Bredesen, D.E., Rosenthal, R.E., Fiskum, G. and Reed, J. (1999) Proc. Natl. Acad. Sci. USA 96, 5752–5757.
[7] Reed, J.C. and Paternostro, G. (1999) Proc. Natl. Acad. Sci. USA 96, 7614–7616.
[8] Martin, J.B. (1999) New Engl. J. Med. 340, 1970–1980.
[9] Schulz, J.B., Weller, M. and Moskowitz, M.A. (1999) Ann. Neurol. 45, 421–429.
[10] Cotman, C.W. and Anderson, A.J. (1995) Mol. Neurobiol. 10, 19–45.
[11] Barinaga, M. (1998) Science 281, 1302–1303.
[12] Vaux, D.L. and Korsmeyer, S.J. (1999) Cell 96, 245–254.
[13] Podack, E.R. (1999) Proc. Natl. Acad. Sci. USA 96, 8312–8314.
[14] Stennicke, H.R. and Salvesen, G.S. (1999) Biochim. Biophys. Acta 1387, 17–31.
[15] Cryns, V. and Yuan, J. (1998) Genes Dev. 12, 1551–1570.
[16] Cohen, G.M. (1997) Biochem. J. 326, 1–16.
[17] Nicholson, D.W. and Thornberry, N.A. (1997) TIBS 22, 299–306.
[18] Braun, J.S., Tuomanen, E.I. and Cleveland, J.L. (1999) Exp. Opin. Invest. Drug 8, 1599–1610.
[19] Wilson, K.P., Black, J.F., Thomson, J.T., Kim, E.K., Griffith, J.P., Navia, M.N., Murcko, M.A., Chambers, S.P., Aldape, R.A., Raybuck, S.A. and Livingston, D.L. (1994) Nature 370, 270–274.
[20] Rotonda, J., Nicholson, D.W., Fazil, K.M., Gallant, M., Gareau, Y., Labelle, M., Peterson, E.P., Rasper, D.M., Ruel, R., Vaillancourt, J.P., Thornberry, N.A. and Becker, J.W. (1996) Nat. Struct. Biol. 3, 619–625.
[21] Mittl, P.R.E., Marco, S.D., Krebs, J.F., Bai, X., Karanewsky, D.S., Priestle, J.P., Tomaselli, K.J. and Grutter, M.G. (1997) J. Biol. Chem. 272, 6539–6547.

[22] Chou, K.C., Jones, D. and Heinrikson, R.L. (1997) FEBS Lett. 419, 49–54.
[23] Watt, W., Koeplinger, K.A., Mildner, A.M., Heinrikson, R.L., Tomasselli, A.G. and Watenpaugh, K.D. (1999) Structure 7, 1135–1143.
[24] Blanchard, H., Kodandapani, L., Mittl, P.R., Macro, S.D., Krebs, J.F., Wu, J.C., Tomaselli, K.J. and Gutter, G. (1999) Structure 7, 1125–1133.
[25] Scaffidi, C., Fulda, S., Srinivassan, A., Friesen, C., Li, F., Tomasselli, K.J., Debatin, K.M. and Krammer, P.H. (1998) EMBO J. 17, 1675–1687.
[26] Li, H., Zhu, H., Xu, C.-J. and Yuan, J. (1998) Cell 94, 491–501.
[27] Li, P., Nijhawan, D., Budihardjo, I., Srinivasula, S.M., Ahmad, M., Alnemri, E.S. and Wang, X. (1997) Cell 91, 479–489.
[28] Qin, H., Srinivasula, S.M., Wu, G., Fernandes-Alnemri, T., Alnemri, E.S. and Shi, Y. (1999) Nature 399, 549–557.
[29] Chou, J.J., Matsuo, H., Duan, H. and Wagner, G. (1998) Cell 94, 171–180.
[30] Luo, X., Budihardjo, I., Zou, H., Slaughter, C. and Wang, X. (1998) Cell 94, 481–490.
[31] Chou, J.J., Li, H., Salvesen, G.S., Yuan, J. and Wagner, G. (1999) Cell 96, 615–624.
[32] Zhou, P., Chou, J.J., Olea, R.S., Yuan, J. and Wagner, G. (1999) Proc. Natl. Acad. Sci. USA 96, 11265–11270.
[33] Kuida, K., Hayadar, T.F., Kuan, C.-Y., Gu, Y., Taya, C., Karasuyama, H., Su, M.S.-S., Rackic, P. and Flavell, R.A. (1998) Cell 94, 325–337.
[34] Hakem, R., Hakem, A., Duncan, G.S., Henderson, J.T., Woo, M., Soengas, M.S., Elia, A., de la Pompa, J.L., Kagi, D., Khoo, W., Potter, J., Yoshida, R., Kaufman, S.A., Kaufman, S.A., Low, S.W., Penninger, J.M. and Mak, T.W. (1998) Cell 94, 339–352.
[35] Duan, H., Orth, K., Chinnaiyan, A.M., Poirier, G.G., Froelich, C.J., He, W.W. and Dixit, V.M. (1996) J. Biol. Chem. 271, 16720–16724.
[36] Srinivasula, S.M., Fernandes-Alnemri, T., Zangrilli, J., Robertson, N., Armstrong, R.C., Wang, L., Trapani, J.A., Tomaselli, K.J., Litwack, G. and Alnemri, E.S. (1996) J. Biol. Chem. 271, 27099–27106.
[37] Altschul, S.F., Gish, W., Miller, W., Myers, E.W. and Lipman, D.J. (1990) J. Mol. Biol. 215, 403–410.
[38] Altschul, S.F., Madden, T.L., Schäffer, A.A., Zhang, J., Zhang, Z., Miller, W. and Lipman, D.J. (1997) Nucleic Acids Res. 25, 3389–3402.
[39] Devereux, J. (1994) The Wisconsin Sequence Analysis Package, Version 8.0, Genetic Computer Group, Madison, WI.
[40] Levitt, M. (1992) J. Mol. Biol. 226, 507–533.
[41] Chou, K.C., Watenpaugh, K.D. and Heinrikson, R.L. (1999) Biochem. Biophys. Res. Commun. 259, 420–428.
[42] Weiner, S.J., Kollman, P.A., Case, D.A., Singh, U.C., Ghio, C., Alagona, G., Profeta Jr., S. and Weiner, P. (1984) J. Am. Chem. Soc. 106, 765–784.
[43] Laskowski, R.A. (1992) ProCheck v.3.4.4, University College, London.
[44] Chothia, C. (1973) J. Mol. Biol. 75, 295–302.
[45] Chou, K.C. and Scheraga, H.A. (1982) Proc. Natl. Acad. Sci. USA 79, 7047–7051.
[46] Chou, K.C., Nemethy, G. and Scheraga, H.A. (1983) Biochemistry 22, 6213–6221.
[47] Chou, K.C. (1995) FEBS Lett. 363, 123–126.
[48] Schechter, I. and Berger, A. (1967) Biochem. Biophys. Res. Commun. 27, 157–162.
[49] Seol, D.W. and Billiar, T.R. (1999) J. Biol. Chem. 274, 2072–2076.
[50] Alnemri, E.S. (1997) J. Cell. Biochem. 64, 33–42.